

See discussions, stats, and author profiles for this publication at: <https://www.researchgate.net/publication/6733939>

# Formation of Solvent Cages around Organometallic Complexes in Thin Films of Supported Ionic Liquid

ARTICLE in JOURNAL OF THE AMERICAN CHEMICAL SOCIETY · DECEMBER 2006

Impact Factor: 12.11 · DOI: 10.1021/ja064204c · Source: PubMed

CITATIONS

40

READS

45

## 5 AUTHORS, INCLUDING:



**Oriol Jimenez**

Technische Universität München

8 PUBLICATIONS 137 CITATIONS

SEE PROFILE



**Thomas Ernst Müller**

RWTH Aachen University

124 PUBLICATIONS 4,192 CITATIONS

SEE PROFILE



**Stefan Steuernagel**

Bruker Corporation

46 PUBLICATIONS 2,197 CITATIONS

SEE PROFILE



**Johannes A Lercher**

Technische Universität München

544 PUBLICATIONS 11,663 CITATIONS

SEE PROFILE

## Formation of Solvent Cages around Organometallic Complexes in Thin Films of Supported Ionic Liquid

Carsten Sievers,<sup>†</sup> Oriol Jimenez,<sup>†</sup> Thomas E. Müller,<sup>\*,†</sup> Stefan Steuernagel,<sup>‡</sup> and Johannes A. Lercher<sup>†</sup>

Lehrstuhl II für Technische Chemie, Technische Universität München, Lichtenbergstrasse 4, 85747 Garching, Germany, and Bruker BioSpin GmbH, Silberstreifen 4, 76287 Rheinstetten, Germany

Received June 26, 2006; E-mail: thomas.mueller@ch.tum.de

Dissolving organometallic complexes in supported films of ionic liquids has recently been introduced as a strategy to immobilize molecular catalysts. This allows fixing molecular catalysts in a widely tailorable environment without the drawbacks of complex grafting chemistry. The first examples appear to be highly promising.<sup>1</sup> The question arises, however, to what extent the highly polar ionic liquid influences the structure and properties of the metal organic complex. Therefore, the detailed characterization of supported films by solid-state NMR spectroscopy<sup>2</sup> was explored for a fully functional catalytic system.

As a case study, we focus on a bifunctional catalyst system.<sup>3</sup> The supported catalyst comprising [Pd(DPPF)(CF<sub>3</sub>CO<sub>2</sub>)<sub>2</sub>]<sup>4</sup> (Lewis acid function) and CF<sub>3</sub>SO<sub>3</sub>H (Brønsted acid function) immobilized in a thin film of imidazolium salts (Figure 1) showed exceptional activity in the addition of aniline to styrene, providing the Markovnikov product *N*-(1-phenylethyl)aniline under kinetic control and the *anti*-Markovnikov product *N*-(2-phenylethyl)aniline under thermodynamic control.

Catalysts were prepared by immobilization of [Pd(DPPF)-(CF<sub>3</sub>CO<sub>2</sub>)<sub>2</sub>] and CF<sub>3</sub>SO<sub>3</sub>H in imidazolium salts (C<sub>3</sub>N<sub>2</sub>H<sub>2</sub>MeRalkyl)<sup>+</sup>-CF<sub>3</sub>SO<sub>3</sub><sup>-</sup> supported on silica. Four different ionic liquids were used, which provide a series of catalysts IL/Pd with decreasing polarity of the ionic liquid (IL) in the sequence EMIm > BMIm > HMIm > HM<sub>2</sub>Im.<sup>4</sup> For comparison, a series of reference samples (IL/H<sup>+</sup>) was prepared, for which only the Brønsted acid CF<sub>3</sub>SO<sub>3</sub>H was supported in the thin film of the ionic liquid.

Analysis of the porosity by nitrogen adsorption showed that the mesopore volume decreased from 0.76 cm<sup>3</sup>·g<sup>-1</sup> (parent support) to ca. 0.13 cm<sup>3</sup>·g<sup>-1</sup> for the supported catalysts. Closer inspection of the isotherm showed that the ionic liquid entirely filled pores with less than 9 nm radius, whereas larger pores remained unaffected. Transmission electron micrographs showed the spherical beads of the fumed silica support (Figure 1). However, the ionic liquid film was much thinner than expected (calculated to 3 nm thick). Thus, the majority of the ionic liquid molecules were not part of an even, physisorbed film on the silica surface, but rather resided in the mesopores. However, in the IR spectra, the SiOH band of the parent silica (3741 cm<sup>-1</sup>) was broadened and shifted to ca. 3320 cm<sup>-1</sup> for the supported catalysts, indicating that all SiOH groups were involved in hydrogen bonding. This proves that the entire silica surface has been covered by ionic liquid. Note that the fact that all SiOH groups are interacting does not allow us to conclude how thick the film is.

The <sup>1</sup>H MAS NMR spectra of the materials were surprisingly well resolved, and the signal for each proton of the imidazolium cation was identified (Figure 2). The additional broad signal is assigned to the acidic proton of CF<sub>3</sub>SO<sub>3</sub>H.

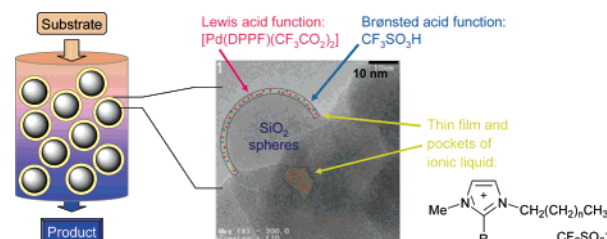


**Figure 1.** Concept of immobilizing organometallic complexes in supported films of ionic liquid (R = H, Me; alkyl = C<sub>2</sub>H<sub>5</sub>, C<sub>4</sub>H<sub>9</sub>, C<sub>6</sub>H<sub>13</sub>) and transmission electron micrograph of the catalyst EMIm/Pd.

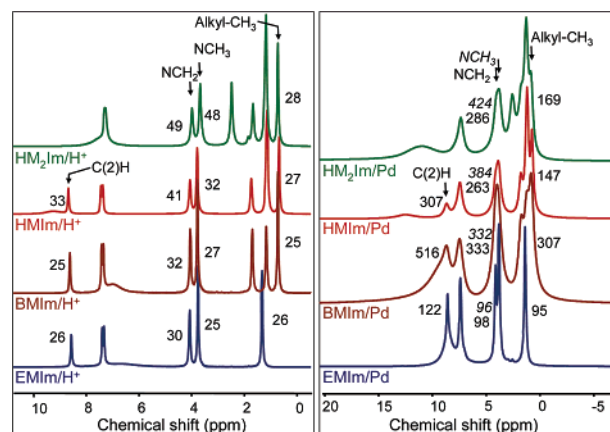


**Figure 2.** <sup>1</sup>H MAS NMR spectra (298 K) of series IL/H<sup>+</sup> (left) and IL/Pd (right) and line widths (Hz) of selected signals.

The line width of the nitrogen-bound methyl and methylene groups increased with increasing size of the imidazolium cation in the order EMIm/H<sup>+</sup> < BMIm/H<sup>+</sup> < HMIm/H<sup>+</sup> < HM<sub>2</sub>Im/H<sup>+</sup> (Figure 2). In NMR spectra of solids, the chemical shift anisotropy is not averaged out by the motion of the molecules, but can be reduced by magic angle spinning (MAS).<sup>5</sup> At frequencies above 5000 Hz, the spectra were independent of rotation speed, indicating that coupling constants to other nuclei in the sample were well below 5000 Hz. Quadrupolar interactions were also insignificant (*I*<sub>H</sub> = 1/2). Differences in *T*<sub>2</sub>, which is not influenced by MAS, thus, were responsible for the changes in line width and can be taken as a measure for the mobility of a particular atomic group.<sup>6</sup> The increase in line width, therefore, shows that the mobility of the aromatic ring decreased with increasing size of the imidazolium cation. On the other hand, the line width of the terminal methyl group in the alkyl side chain was equal (25–28 Hz), showing that the flexibility of the alkyl group was not influenced by the size of the cation.

A large increase of the line width was observed when [Pd(DPPF)-(CF<sub>3</sub>CO<sub>2</sub>)<sub>2</sub>] and CF<sub>3</sub>SO<sub>3</sub>H were immobilized in the supported ionic

<sup>†</sup> Technische Universität München.

<sup>‡</sup> Bruker BioSpin GmbH.

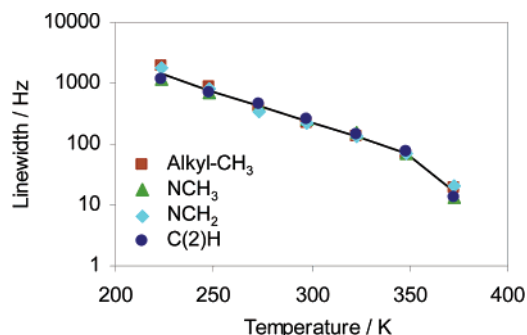


**Figure 3.** Temperature dependence of the line width of selected protons in the  $^1\text{H}$  MAS NMR spectra of EMIm/Pd.

liquids (Figure 2). This suggests a substantial decrease in the mobility of the imidazolium cations. Reference samples prepared by dissolution of  $[\text{Pd}(\text{DPPF})(\text{CF}_3\text{CO}_2)_2]$  and  $\text{CF}_3\text{SO}_3\text{H}$  in the parent ionic liquids showed a large increase in viscosity compared to that in the parent ionic liquid,<sup>7</sup> confirming that the mobility of the molecules was considerably lowered.

The position of the NMR signals was equal in the two series IL/ $\text{H}^+$  and IL/Pd (within  $\pm 0.1$  ppm). Note that the molar ratio of  $\text{Pd}^{2+}$ , DPPF,  $\text{CF}_3\text{SO}_3\text{H}$ , and ionic liquid in the catalysts was 1:1.5:2.5:25–33. A single peak with Lorentzian shape was observed for each proton of the imidazolium cations in the series IL/Pd. This indicates that the ionic liquid did not coordinate directly to the palladium center in  $[\text{Pd}(\text{DPPF})(\text{CF}_3\text{CO}_2)_2]$  and that all ionic liquid molecules in the supported film were on average equally affected by the presence of the palladium complex. Rapid exchange of coordinated and free imidazolium cations could be excluded by variable temperature NMR spectra (vide infra).

In  $^{31}\text{P}$  MAS NMR spectroscopy, the signal due to the phosphine ligand of the palladium complex was observed at 47.3 ppm with a relatively large line width of 440–1360 Hz. In comparison, the  $^{31}\text{P}\{^1\text{H}\}$  NMR signal for a solution of  $[\text{Pd}(\text{DPPF})(\text{CF}_3\text{CO}_2)_2]$ ,  $\text{CF}_3\text{SO}_3\text{H}$ , and IL in  $\text{CD}_2\text{Cl}_2$  was observed at 47.1 ppm with a much smaller line width of 2.5 Hz. This suggests that the mobility of the palladium complexes in the supported ionic liquid was also restricted. To explain these observations, we propose that the imidazolium cations form a solvent cage around the palladium complexes, thereby establishing a long-range ordered system,<sup>8</sup> which in turn is responsible for the reduced mobility.

Similar to the IL/ $\text{H}^+$  series, the line width of the nitrogen-bound methyl and methylene group in the  $^1\text{H}$  MAS NMR spectra was significantly higher than that of the terminal methyl group of the alkyl chain (Figure 2). A maximum in the line width of the  $\text{N}-\text{CH}_2$  and the  $\text{alkyl}-\text{CH}_3$  groups was observed for BMIm/Pd. In particular, the line width of the methyl group in the hexyl chain was much lower than that in the butyl chain. This suggests that the first four carbon atoms of the alkyl chains contribute most to the intermolecular interactions between the IL and the palladium complexes. We speculate that hydrophobic interactions between the alkyl chain and the aromatic rings of the phosphine ligand lead to domain formation.<sup>9</sup> Thus, the line width in the NMR spectra provides a measure for where these interactions are most significant.

The dynamic interaction of ionic liquid and the Pd complex was investigated in further detail by temperature-resolved MAS NMR experiments. For all samples, the line width of all peaks decreased exponentially with temperature. A change of slope in the logarithmic plot shows that a phase transition from glassy to liquid state occurred at ca. 348 K for EMIm/Pd and BMIm/Pd (Figure 3). For HMIm/Pd, the phase transition occurred above 373 K. After the

phase transition, the line width in the spectra of the IL/Pd samples was similar to that of the IL/ $\text{H}^+$  series at 298 K.

We speculate that the solvent cages are formed by disruption of interionic interactions between the ionic liquid anions and cations during dissolution of the palladium complexes. This, in turn, causes the local structure of the ionic liquid to break down.<sup>10</sup> In an attempt to minimize the potential energy, the spheres of ionic liquid molecules around the complexes assume a minimum size. It is estimated, based on the molar ratio of complex to ionic liquid and the fact that only one set of signals was observed in the NMR spectra, that the supramolecular aggregates consist of one complex molecule and up to 25–33 ion pairs of the ionic liquid. The aggregates arrange to a regular packing with glass-like structure. At the phase transition, the solvent cages break down and the molecules acquire mobility similar to that of the parent supported liquid, which does not contain the dissolved complex.

The present report is the first experimental evidence for the formation of ordered three-dimensional structures in solutions of organometallic complexes in a thin film of supported ionic liquid. The ordering effect leads to a drastically reduced mobility of ionic liquid and complex molecules and could be used to induce unusual properties in the supported complexes. Possible applications include the enhancement of metal–substrate interactions, the reorientation of substrate molecules within in the solvent cage during a two-step catalytic process, and the possibility of directing the approach of molecules to catalytically active centers.

**Acknowledgment.** The authors are grateful to Max-Buchner-Stiftung for partial support in the form of a fellowship for O.J. TEM micrographs and BET measurements were performed by M. Neukamm. Neutron activation measurements were done by X. Lin and B. Wierczinski, Institut für Radiochemie. The authors acknowledge fruitful discussions in the framework of the network of excellence IDECAT.

**Supporting Information Available:** Details of catalyst preparation, three figures (NMR spectra of EMIm, temperature and spinning frequency dependent  $^1\text{H}$  MAS NMR spectra of EMIm/Pd), and four tables (catalyst preparation, BET surface area and pore volume, chemical shifts of IL/ $\text{H}^+$ , IL/Pd, and reference compounds). This material is available free of charge via the Internet at <http://pubs.acs.org>.

## References

- (a) Welton, T. *Coord. Chem. Rev.* **2004**, *248*, 2459. (b) Breitenlechner, S.; Fleck, M.; Müller, T. E.; Suppan, A. *J. Mol. Catal. A* **2004**, *214*, 175. (c) Riisager, A.; Wasserscheid, P.; Hal, R.; Fehrmann, R. *J. Catal.* **2003**, *219*, 452. (d) Mehnert, C. P.; Cook, R. A.; Dispenziere, N. C.; Afeworki, M. *J. Am. Chem. Soc.* **2002**, *124*, 12932. (e) Hagiwara, H.; Sugawara, Y.; Isobe, K.; Hoshi, T.; Suzuki, T. *Org. Lett.* **2004**, *6*, 2325.
- For a solid-state NMR study on adsorption, see: Tao, T.; Pan, V. H.; Zhou, J.-W.; Maciel, G. E. *Solid State Nucl. Magn. Reson.* **2000**, *17*, 52.
- Jimenez, O.; Müller, T. E.; Sievers, C.; Spirkel, A.; Lercher, J. A. *Chem. Commun.* **2006**, 2974.
- DPPF = 1,1'-bis(diphenylphosphino)ferrocene, EMIm = 1-ethyl-3-methylimidazolium trifluoromethane sulfonate, BMIm = 1-butyl-3-methylimidazolium trifluoromethane sulfonate, HMIm = 1-hexyl-3-methylimidazolium trifluoromethane sulfonate, HM<sub>2</sub>Im = 1-hexyl-2,3-dimethylimidazolium trifluoromethane sulfonate.
- Laws, D. D.; Bitter, H.-M. L.; Jerschow, A. *Angew. Chem., Int. Ed.* **2002**, *41*, 3096 and references therein.
- (a) Lauenstein, A.; Tegenfeldt, J. *J. Phys. Chem. B* **1997**, *101*, 3311. (b) Johansson, A.; Tegenfeldt, J. *J. Chem. Phys.* **1996**, *104*, 5317. (c) Spindler, R.; Shriver, D. F. *J. Am. Chem. Soc.* **1988**, *110*, 3036.
- Bonhôte, P.; Dias, A. P.; Papageorgiou, N.; Kalyanasundaram, K.; Gratzel, M. *Inorg. Chem.* **1996**, *35*, 1168.
- Self-assembly of ionic liquids has been reported by: (a) Atkin, R.; Warr, G. G. *J. Am. Chem. Soc.* **2005**, *127*, 11940. (b) Mantz, R. A.; Trulove, P. C.; Carlin, R. T.; Osteryoung, R. A. *Inorg. Chem.* **1995**, *34*, 3846.
- Wang, Y. T.; Voth, G. A. *J. Am. Chem. Soc.* **2005**, *127*, 12192.
- Crowhurst, L.; Lancaster, N. L.; Arlandis, J. M. P.; Welton, T. *J. Am. Chem. Soc.* **2004**, *126*, 11549.

JA064204C

## Supplementary

**Catalyst preparation** The palladium complex was prepared in situ following a published procedure.<sup>1</sup> For catalysts IL/Pd, CF<sub>3</sub>SO<sub>3</sub>H (for quantities see Table S1) was dissolved in 1-alkyl-3-methyl-imidazolium trifluoromethane sulphonate with alkyl = ethyl (EMIm), butyl (BMIm), hexyl (HMIm) or molten 1-hexyl-2,3-dimethyl-imidazolium trifluoromethane sulphonate (HM<sub>2</sub>Im). A solution of Pd(CF<sub>3</sub>CO<sub>2</sub>)<sub>2</sub> and 1,1'-bis(diphenylphosphino)-ferrocene (DPPF) in CH<sub>2</sub>Cl<sub>2</sub> was added and the mixture stirred for 10 min. Silica (Aerosil 355 by Degussa, 150 m<sup>2</sup>/g) was ground to particle size 60-200 µm and added to the mixture. The suspension was stirred for 10 min, then frozen rapidly and the volatiles were removed in a partial vacuum, while the sample was warming slowly to RT. A free flowing powder was obtained. For reference, a series of catalysts IL/H<sup>+</sup> was prepared without palladium complex.

**Table S1** Amounts used in the preparation of the supported material IL/Pd and IL/H<sup>+</sup>.

Ionic liquid	Ionic liquid / ml	Pd(CF <sub>3</sub> CO <sub>2</sub> ) <sub>2</sub> / mg	DPPF / mg	CF <sub>3</sub> SO <sub>3</sub> H / mg	Silica / g
EMIm	2.5	—	—	150	5.0
	2.5	133	333	150	5.0
BMIm	2.5	—	—	150	5.0
	2.5	133	333	150	5.0
HMIm	2.5	—	—	150	5.0
	2.5	133	333	150	5.0
HM <sub>2</sub> Im	2.5 <sup>a</sup>	—	—	150	5.0
	2.5 <sup>a</sup>	133	333	150	5.0

<sup>a</sup> HM<sub>2</sub>Im is solid at RT, a molten sample was used.

**Catalyst characterization** The pore structure was analyzed by nitrogen adsorption at 77 K on a PMI Automated BET Sorptometer (Table S2). The palladium content in the supported catalysts was determined by neutron activation (Table S2). For TEM of EMIm/Pd, the sample was ground, suspended in hexane and dispersed using an ultrasonic bath. Drops of the dispersion were applied to a copper grid-supported carbon film. A JEM-2010 Jeol transmission electron microscope operating at 120 kV was used.

**Table S2** Data of catalyst characterization.

Sample	BET surface area / m <sup>2</sup> ·g <sup>-1</sup>	Pore volume / cm <sup>3</sup> ·g <sup>-1</sup>	Pd contents / mmol·g <sup>-1</sup>
SiO <sub>2</sub>	142	0.76	—
EMIm/H <sup>+</sup>	22	0.15	—
BMIm/H <sup>+</sup>	20	0.13	—
HMIm/H <sup>+</sup>	23	0.18	—
HM <sub>2</sub> Im/H <sup>+</sup>	22	0.15	—
EMIm/Pd	13	0.10	0.037
BMIm/Pd	12	0.09	0.038
HMIm/Pd	20	0.15	0.040
HM <sub>2</sub> Im/Pd	15	0.10	0.039

For the NMR measurements, the samples were pressed into ZrO<sub>2</sub> rotors and spun at 10 kHz (except where noted otherwise). The <sup>1</sup>H MAS NMR measurements were performed on a Bruker AV600 spectrometer (B<sub>0</sub> = 14.1 T). For cooling the bearing and drive gas stream were sent through a heat exchanger in liquid nitrogen. The spectra were recorded as the sum of 16 scans using single pulse excitation with a pulse length of 2.6 µs and recycle time of 3 s. The spectra were referenced to an external adamantane standard (δ<sub>H</sub> = 1.78 ppm). A comparison of the room temperature NMR spectra of pure EMIm (where the NMR tube contained a capillary filled with CD<sub>2</sub>Cl<sub>2</sub> as reference), EMIm/H<sup>+</sup> and EMIm/Pd

is provided in Figure S1. The influence of the spinning rate is demonstrated in Figure S2. Variable temperature <sup>1</sup>H MAS NMR spectra of EMIm/Pd are given in Figure S3. The chemical shifts of selected signals in the <sup>1</sup>H NMR spectra of IL/H<sup>+</sup> and IL/Pd are summarized in Table S3.

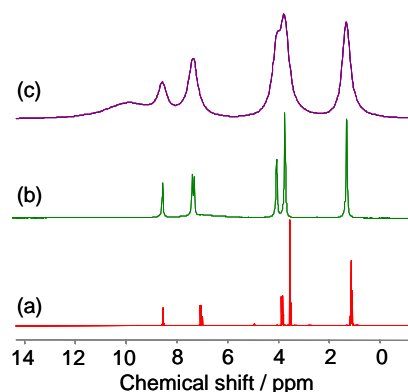


**Figure S1.** Comparison of the room temperature NMR spectra of (a) EMIm dissolved in CD<sub>2</sub>Cl<sub>2</sub>, (b) EMIm/H<sup>+</sup> and (c) EMIm/Pd

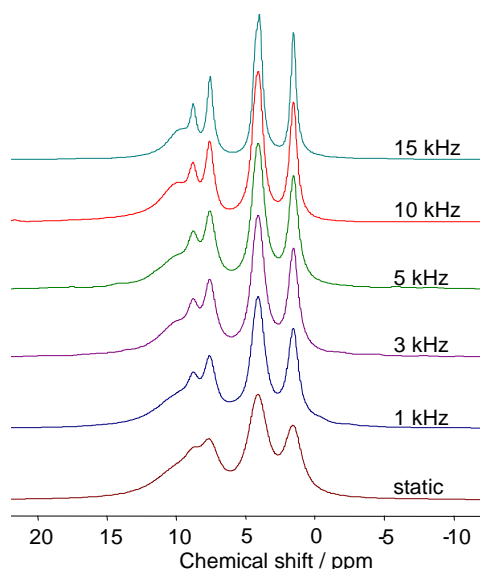


**Figure S2.** Influence of the spinning rate on the <sup>1</sup>H NMR spectrum of EMIm/Pd.

**Table S3** Chemical shifts and assignment for selected imidazolium and acid protons in IL/H<sup>+</sup> and IL/Pd at 298 K.

Sample	C(2)-H	N-CH <sub>2</sub>	N-CH <sub>3</sub>	Alkyl-CH <sub>3</sub>	H <sup>+</sup>
EMIm/H <sup>+</sup>	8.59	4.10	3.77	1.35	6.69
BMIm/H <sup>+</sup>	8.64	4.07	3.80	0.75	7.01
HMIm/H <sup>+</sup>	8.70	4.08	3.81	0.71	9.28
HM <sub>2</sub> Im/H <sup>+</sup>	-	4.01	3.70	0.75	7.30
EMIm/Pd	8.54	4.08	3.76	1.34	8.06
BMIm/Pd	8.65	4.08	3.79	0.79	9.16
HMIm/Pd	8.64	4.07	3.77	0.70	12.05
HM <sub>2</sub> Im/Pd	-	4.03	3.70	0.81	10.91

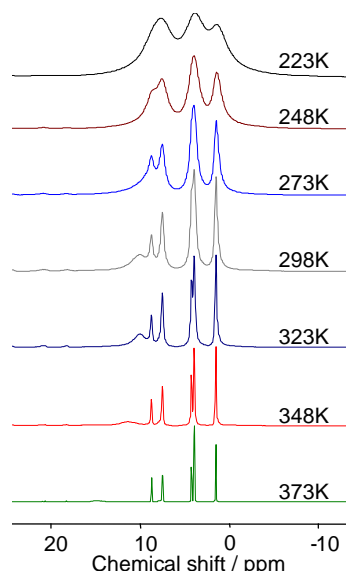


**Figure S3.** Variable temperature  $^1\text{H}$  MAS NMR spectra of the catalyst EMIm/Pd.

The  $^{31}\text{P}$  MAS NMR measurements were performed on a Bruker AV500 spectrometer ( $B_0 = 11.7$  T). The spectra were recorded as the sum of 5000 scans using a proton decoupling pulse sequence with a pulse length of  $2.5\ \mu\text{s}$  and recycle time of 5 s. The spectra were referenced to an external  $(\text{NH}_4)_2\text{HPO}_4$  standard ( $\delta_{\text{P}} = 1.11$  ppm).

**Reference samples for NMR spectroscopy** Samples were prepared by dissolving  $\text{CF}_3\text{SO}_3\text{H}$  in EMIm, BMIm or HmIm (amounts 1/10 of those in Table S1). A solution of  $\text{Pd}(\text{CF}_3\text{CO}_2)_2$  and 1,1'-bis(diphenylphosphino)ferrocene (DPPF) in 10 ml  $\text{CH}_2\text{Cl}_2$  was added and the solution stirred for 10 min. The volatiles were removed in a partial vacuum. One drop of the viscous liquid was dissolved in  $\text{CD}_2\text{Cl}_2$ .  $^{31}\text{P}\{^1\text{H}\}$  NMR spectra were recorded on a Bruker AV250 spectrometer ( $B_0 = 5.8$  T) as the sum of 32 scans using a single pulse excitation sequence with a pulse length of  $2.5\ \mu\text{s}$  and recycle time of 2 s. For all samples, a single NMR signal was observed at 47.1 ppm with 2.5 Hz line width.

**Palladium complex** The chemical shifts in  $^{31}\text{P}\{^1\text{H}\}$  NMR are in the expected range for mononuclear complexes containing the chelating diphosphine ligand BINAP (see Table S4). Note that all  $^{31}\text{P}$  NMR spectra were taken close to working conditions of the catalyst (mixture of anions  $\text{CF}_3\text{CO}_2^-$  and  $\text{CF}_3\text{SO}_3^-$ , ratio  $\text{Pd}^{2+}/\text{DPPF}$  1/1.5, acidic conditions).

**Table S4** Chemical shifts in  $^{31}\text{P}\{^1\text{H}\}$  NMR for reference compounds.

Phosphine / Complex	Solvent	$\delta$ / ppm	Reference
DPPF	$\text{CH}_2\text{Cl}_2$	-16.8	2
$[\text{Pd}(\text{DPPF})\text{Cl}_2]$	$\text{CH}_2\text{Cl}_2$	34.0	2
$[\text{Pd}(\text{DPPF})(\text{CF}_3\text{CO}_2)_2]$	$\text{CDCl}_3$	36.2	3

## References

- 1 Kawatsura, M.; Hartwig, J. F. *J. Am. Chem. Soc.* **2000**, *122*, 9546.
- 2 Corain, B.; Longato, B.; Favero, G.; Ajo, D.; Pilloni, G.; Russo, U.; Kreissl, F. R. *Inorg. Chim. Acta* **1989**, *157*, 259.
- 3 Neo, Y. C.; Yeo, J. S. L.; Low, P. M. N.; Chien, S. W.; Mak, T. C. W.; Vittal, J. J.; Hor, T. S. A. *J. Organomet. Chem.* **2002**, *658*, 159.